이학석사 학위논문

보리코나졸의 Therapeutic Drug Monitoring을 위한 최적의 채혈시각 탐색을 위한 시뮬레이션 연구

Simulation Study to Explore Optimal Sampling Time for Therapeutic Drug Monitoring of Voriconazole

울 산 대 학 교 대 학 원

의 과 학 과

최 승 찬

Simulation Study to Explore Optimal Sampling Time for Therapeutic Drug Monitoring of Voriconazole

지 도 교 수　　임 형 석

이 논문을 이학석사 학위 논문으로 제출함

2022년　　2월

울 산 대 학 교 대 학 원

의 과 학 과

최 승 찬

최승찬의 이학석사학위 논문을 인준함

심사위원 배 균 섭 (인)

심사위원 임 형 석 (인)

심사위원 최 병 문 (인)

울 산 대 학 교 대 학 원

2022년 2월

Abstract

Objective: Voriconazole is a broad-spectrum triazole antifungal agent with activity against a wide range of yeasts and filamentous fungi which has been approved worldwide for invasive fungal infections. It has a narrow therapeutic range, nonlinear pharmacokinetic profile, and high interindividual variability. Area under the time-concentration curve during 12-hour dosing interval (AUC_{0-12}) and pre-dose concentration (C_{trough}) are clinically important variables based on which dose adjustment is made. The purpose of this study is to explore optimal sampling time for therapeutic drug monitoring of voriconazole.

Methods: Plasma voriconazole concentrations following three dosing regimens (Scenario 1, loading dose of 6 mg/kg IV q12hr on day 1, followed by maintenance dose of 4 mg/kg IV q12hr; Scenario 2, loading dose of 6 mg/kg IV q12hr on day 1, followed by 3 mg/kg IV q12hr; Scenario 3, loading dose of 6 mg/kg IV q12h on day 1, followed by 200 mg PO q12hr) were simulated to generate 1,000 sets of data for each scenario using NONMEM® (version 7.4.4). Using one or two concentration data early after the initiation of therapy, plasma concentration over time, AUC_{0-12}, and C_{trough} at steady state of each individual were predicted by maximum a posteriori (MAP) method. By comparing the accuracy and precision of these values, the optimal pharmacokinetic (PK) sampling time was explored. During the MAP prediction, deviation in sampling time from the planned time was also taken into account.

Results: Plasma voriconazole concentration over time was well predicted by MAP method for all of the sampling times explored in this study with minimal bias (less than 10%). However, precision of predicted concentration was different by time points used in MAP, with low precision especially for the concentration around mid-point of the dosing interval. AUC_{0-12} was best predicted with high accuracy and precision using concentration at 2- or 3-hour sampling time in scenario 1 and 2. In scenario 3, AUC_{0-12} was well predicted with similar accuracies across all the sampling times of 1 through 12 hours, but the precision was predicted to be high when using later time points near 12 hour.

Conclusions: We successfully reconstructed a voriconazole PK model and conducted a simulation study. The simulation suggested optimal sampling time points that can be implemented in clinical setting for the therapeutic drug monitoring of voriconazole. The current study provides useful information for individualized, optimal therapy of voriconazole.

Table of Contents

List of Tables

List of Figures

List of Appendix

Introduction

Invasive fungal infections (IFIs) have risen in a number of immunocompromised patients, those receiving chemotherapy for neoplastic diseases, those on immunosuppressants for certain medical conditions such as solid organ or bone marrow transplantation, premature birth, advanced age, and acquired immunodeficiency syndrome (AIDS)(1, 2). IFI is related with morbidity and mortality in immunocompromised patients and the incidence of IFI has increased dramatically in recent years (3-5). The well-known causative organisms of IFI include Aspergillus spp., Candida spp., Fusarium spp., Scedosporium spp., and Penicillium spp., among which Aspergillus spp. is the most common mould causing IFI in immunocompromised patients (3, 6).

Voriconazole is a synthetic second-generation, broad-spectrum triazole derivative of fluconazole. Voriconazole exerts its pharmacological effect by inhibiting the cytochrome P450 (CYP)-dependent enzyme 14- α-sterol demethylase, thereby disrupting cell membrane and halting fungal growth. Voriconazole is rapidly absorbed within 2 hours after oral administration and oral bioavailability is as high as more than 90%, which is why voriconazole formulation can be switched between oral and intravenous ones when clinically appropriate (6). In the US and Europe, recommended dose are the same for both oral and intravenous ones but the patient's source of infection and ages are different. Voriconazole is potent against a broad spectrum of clinically significant pathogens, including Aspergillus, Candida, Cryptococcus, Fusarium, and Scedosporium.

Voriconazole has nonlinear PK profile in adult patients at risk of aspergillosis but exhibits linear PK in children. Voriconazole's PK profile has high variability between and within individuals, caused by many factors such as age, sex, race, genotype variation, liver dysfunction and presence of food. Voriconazole undergoes significant metabolism by CYP2C19, CYP3A4, and CYP2C9 with a high affinity for CYP2C19 (7). Genetic polymorphisms in CYP2C19 are associated with 30 ~ 50 % variation in voriconazole metabolism among individuals.

Voriconazole has narrow therapeutic range and high variation in blood concentration. Therefore, ensuring the drug concentration within a specified range by measuring drug concentration in biologic fluid in each subject would be helpful for optimal, individualized therapy of voriconazole. Therapeutic drug monitoring (TDM) for voriconazole is supported and recommended by both U.S. Food and Drug Administration (FDA) and the Infectious Diseases Society of America (IDSA) (8, 9). TDM for voriconazole has been used to optimize dosing regimen for improvement of therapeutic effect of voriconazole and prevention of toxicity related with voriconazole in each individual.

This study is a simulation study based on a previously reported population PK model for voriconazole, to explore the optimal PK sampling time(s) for Bayesian prediction of voriconazole PK in TDM. This study aimed to identify sampling time by evaluating the predictabilities of MAP method for voriconazole PK by comparing the model-predicted PK using sparse concentration with various sampling times and simulated true PKs in terms of accuracy and precision. An overall flow of this study is provided in Figure 1, and detailed information is given in the following subsections.

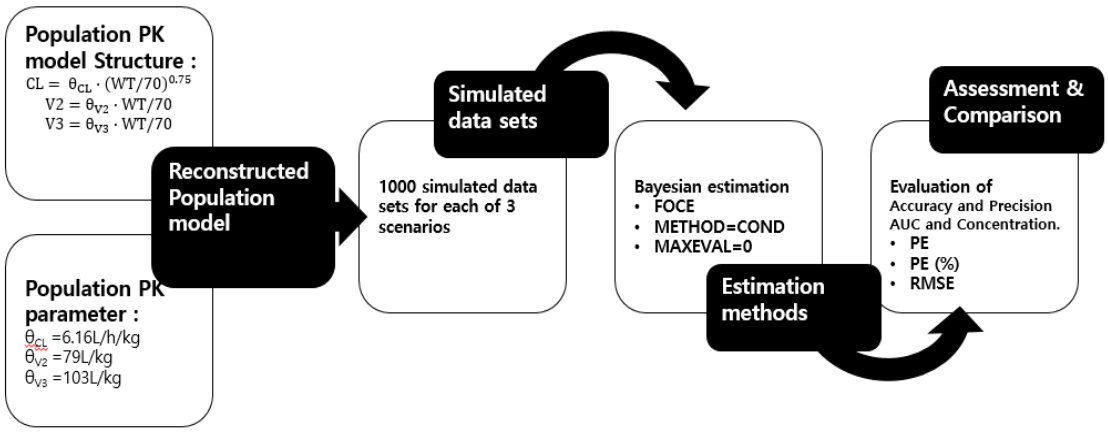

Figure 1. Scheme of the study design

Different steps of the study are outlined in the figure.

Methods

We searched previous publications on PK analysis of voriconazole which used NONMEM software and then selected an article that included PK model structure and parameters. PK model for voriconazole was reconstructed in NONMEM based on the previously reported population PK models for voriconazole (4, 5). Using the reconstructed PK model, plasma voriconazole concentrations over time following three dosing regimens consisting of loading doses in adult population were simulated (1,000 data sets for each regimen) using NONMEM. Residual errors as well as interindividual variability were reflected in the simulation. Each set of data represented observed concentrations in each hypothetical individual. Using one or two simulated concentrations during loading period in each set of data, plasma concentration over time, area under the time-concentration curve during 12-hour dosing interval ($AUC_{0\text{-}12}$), and pre-dose concentration (C_{trough}) at steady state were predicted by maximum a posteriori (MAP) method(10). Residual variabilities were not reflected during the Monte-Carlo simulation. These predictions represented predicted values for each hypothetical individual. The predicted PK values of voriconazole were compared with simulated PK values to determine the accuracy and precision of predictions among dosing regimens and PK sampling time(s).

Literature-based Reconstruction of a Population PK Model for Voriconazole

Reference PK model for voriconazole used in the simulation and MAP prediction is a two-compartment model with first-order absorption and mixed linear (first-order) and nonlinear (Michaelis-Menten; time-dependent V_{max}) elimination developed for intravenous and oral data in children, adolescents, and adults (Fig.2). Reference population PK model for voriconazole was constructed using NONMEM (version 7.1.2; Icon Development Solutions, Ellicott City, MD) with ADVAN 13 subroutine and FOCE method on log-transformed concentrations. Interindividual variability was modeled using exponential additive to a logit scale. Residual error model was additive error on the log-transformed concentration.

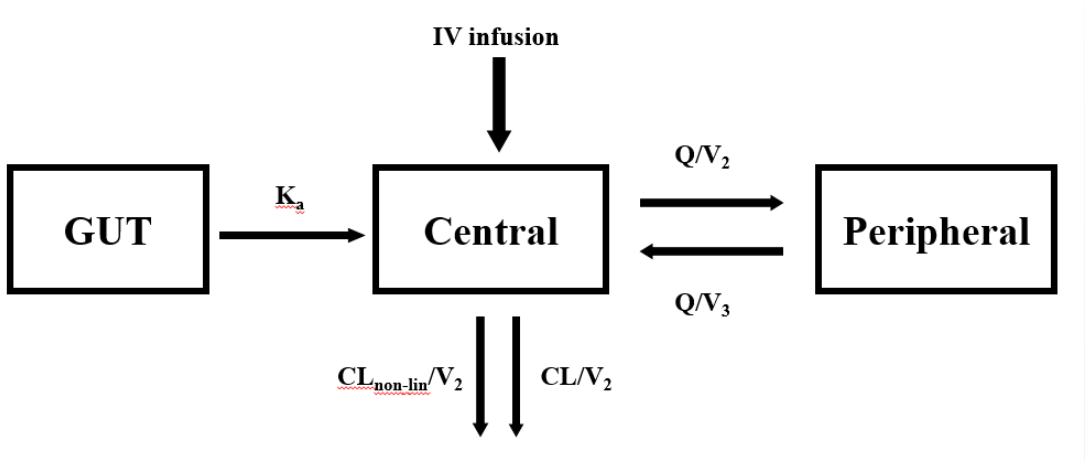

Figure 2. Referenced population PK model for voriconazole

$K_m is\ the\ Michaelis-Menten\ constant; CL\ is\ linear\ clearance;$

$V2\ is\ the\ central\ volume\ of\ distribution; V3\ is\ the\ peripheral\ volume\ of\ distribution;$

$Q\ is\ intercompartmental\ clearance;\ F_1 is\ oral\ bioavailability;$

$K_a is\ the\ first-order\ absorption\ rate\ constant;\ A_{lag}\ is\ absorption\ lag\ time;$

$\theta is\ the\ estimated\ of\ fixed\ effect\ in\ NONMEM$

Two-compartment model with first-order absorption and mixed linear (first-order) and nonlinear (Michaelis-Menten and time-dependent V_{max}) elimination used to fit voriconazole IV and oral data. CL_{nonlin}, nonlinear clearance $V_{max}/ (C_p + K_m)$, where V_{max} is the time-dependent maximum elimination rate, C_p is the plasma voriconazole concentration, and K_m is the Michaelis-Menten constant.

The equations implemented in this model are as follows.

$$K_m = \theta_{Km} \cdot (1 + \theta_{STDY1,ped} \cdot STDY_{1,ped})$$

$$V_{max} = V_{max,1} \cdot (1 - V_{max,inh} \cdot \frac{(T-1)}{(T-1) + (T_{50} - 1)})$$

Where V_{max} was allowed to reduce from an initial value with time (T). To increase the model stability, as well as the interpretability of model parameters, the V_{max} function was parameterized so that V_{max} at 1 h ($V_{max,\ 1}$) was the parameter estimated, since there were no PK samples providing information on V_{max} at time zero. The reduction in V_{max} over time was best described by an inhibitory function with a maximum fraction of the inhibition ($V_{max,\ inh}$). T_{50} described the time in hours after initiation of dosing,

where half of the maximum inhibition occurred. $V_{max,\ inh}$ is 100% if an adult is a CYP2C19 heterozygous extensive metabolizer (HEM) or poor metabolizer (PM).

$$V_{max,1} = \theta_{Vmax,1} \cdot \left(\frac{WT}{70}\right)^{0.75} \cdot (1 + \theta_{STDY1,ped} \cdot STDY_{1,ped})$$

$$\text{logit}(V_{max,inh}) = \theta_{Vmax,inh} + \theta_{\text{AGE<12}} \cdot (\text{AGE} < 12)$$

$$T_{50} = \theta_{T50}$$

$$\text{CL} = \theta_{CL} \cdot (WT/70)^{0.75}$$

$$\text{V2} = \theta_{V2} \cdot WT/70$$

$$\text{V3} = \theta_{V3} \cdot WT/70$$

$$\text{Q} = \theta_{Q} \cdot \left(\frac{WT}{70}\right)^{0.75} \cdot (1 + \theta_{QnotSTDY5,adult} \cdot (1 - STDY_{5,adult}))$$

$$\text{logit(F1)} = \theta_{F1}$$

$$k_a = \theta_{ka} \cdot (1 + \theta_{STDY4,adol} \cdot STDY_{4,adol}) \cdot (1 - STDY_{5,adult}) + \theta_{STDY5,adult} \cdot STDY_{5,adult}$$

$$A_{lag} = \theta_{ka} \cdot (1 + \theta_{AlagnotSTDY5,adult} \cdot (1 - STDY_{5,adult}))$$

Table 1. Voriconazole population PK parameter estimates for the reconstructed model

Parameter	Typical value	Interindividual variability	SD
K_m (μg/ml)		$K_{m,i} = K_m \cdot \exp(\eta_{Km} \cdot V_{max,1})$	
θ_{Km}/ $\theta_{STDY1,ped}$	1.15 /− 0.382	$\omega_{Km} \cdot V_{max,1}$	1.36
$V_{max,1}$ (μg/h/70 kg[c])		$V_{max,1,i} = V_{max,1} \cdot \exp(\eta_{Km-Vmax,1} \cdot V_{max,scale})$	
$\theta_{Vmax,1}$	114	$\omega_{Km} \cdot V_{max,1}/\omega_{Vmax1,ped}$	1.36 / 0.239
$\theta_{STDY1,ped}$	− 0.382	$\theta_{Vmax,scale.adol}$	0.208
		$\theta_{Vmax,scale.adult}$	0.584
$V_{max,inh}$			
$\theta_{Vmax,inh}$/ $\theta_{AGE<12}$	1.50 / −0.39		
T_{50} (h)			
θ_{T50}	2.41		
CL (liter/h/70 kg[c])		$CL,i = CL \cdot \exp(\eta_{CL} \cdot (1 + \theta_{\eta CL.notSTDY5,adult} \cdot notSTDY_{5,adult}))$	
θ_{CL}	6.16	ω_{CL} / $\theta_{\eta CL.notSTDY5,adult}$	0.435 / 1.70
V2(liters/70 kg[c])		$V_{2,i} = V_2 \cdot \exp(\eta_{V2})$	
θ_{V2}	79.0	ω_{V2}	0.136
V3(liters/70 kg[c])		$V_{3,i} = V_3 \cdot \exp(\eta_{V3})$	
θ_{V3}	103	ω_{V3}	0.769
Q (liters/h/70 kg[c])		$Q,i = Q \cdot \exp(\eta_Q)$	
θ_Q/ $\theta_{QnotSTDY5,adult}$	15.5 / 0.637	ω_Q	0.424
F_1		$\text{logit}(F_{1,i}) = \text{logit}(F_1) + ETATR,i$	
θ_{F1}	0.585	$\omega_{FnotSTDY5,adult}$	1.67
		$\omega_{FSTDY5,adult}$	0.686
		θ_{BC-F}	0.367
K_a (h^{-1})		$K_{a,i} = K_a \cdot \exp(\eta_{K_a} \cdot notSTDY_{5,adult})$	
θ_{Ka} / $\theta_{STDY4,adol}$	1.19 / - 0.615	ω_{Ka}	0.898
$\theta_{STDY5,adult}$	100 FIX		
Alag(h)			
θ_{Alag}/ $\theta_{QnotSTDY5,adult}$	0.949 / - 0.874		
Residual error	$W^h = \theta_{STDY1,ped} \cdot STDY_{1,ped} + \theta_{STDY2,ped} \cdot STDY_{2,ped} + \theta_{STDY3,4,ped,adol} \cdot STDY_{3,4,ped,adol} + SQRT(\theta_{STDY5,adult}^2 \cdot \theta_{STDY5,adult,oral}^2, Oral) \cdot STDY_{5,adult}$		
$\theta_{STDY1,ped}$	0.593	$\theta_{STDY5,adult}$	0.0912
$\theta_{STDY2,ped}$	0.425	$\theta_{STDY5,adult,oral}$	0.132
$\theta_{STDY3,4,ped,adol}$	0.365		
$W,i = W \cdot \exp(\eta_{RE} \cdot notSTDY_{5,adult})$			
ω_{RE}	0.456		

[a] SD, standard deviation of random effects (ω)

[b] Note that a power function of 0.75 was applied for clearance terms, i.e., the relationship to weight is not linear

[c] $V_{max,inh} = \exp(\theta_{Vmax,1} \quad \theta_{STDY1,ped})/(1+\exp(\theta_{Vmax,1} \quad \theta_{STDY1,ped}))$. $V_{max,inh}$ = 100% if the adult is a CYP2C19 HEM or PM

[d] $V_{max,1}, i \quad = V_{max,1} \cdot \exp(\eta_{Vmax,1.ped} \cdot STDY_{1-3,ped} + \eta_{Km-\ Vmax,1} \cdot \theta_{vmax,scale,adol} \cdot STDY_{4,adol} + \eta_{Km-\ Vmax,1} \cdot \theta_{vmax,scale,adult} \cdot STDY_{5,adult})$.

[e] Box-Cox transformation. $ETART, i^{\theta BC-F} - \frac{1}{\theta_{BC-F}}; EXPETA, i = \exp(\eta_{FnotSTDY5,adult}) \cdot notSTDY_{5,adult} + \exp(\eta_{FSTDY5,adult}) \cdot STDY_{5,adult}$

[f] NS, not supported model.

[g] W, standard deviation of residual error (on a log scale).

Monte Carlo simulation

Plasma voriconazole concentration following three dosing regimens (Scenario 1, loading dose of 6 mg/kg IV q 12hr on day 1, followed by maintenance dose of 4 mg/kg IV q 12hr; Scenario 2, loading dose of 6 mg/kg IV q 12hr on day 1, followed by 3 mg/kg IV q 12hr; Scenario 3, loading dose of 6 mg/kg IV q 12hr on day 1, followed by 200 mg PO q 12hr) were simulated with 1,000 replicates for each scenario using NONMEM. In Monte-Carlo simulations, random variables were generated at the covariate levels either from log normal distribution (continuous covariate) or from uniform distribution (binary categorical covariate) except for age which was fixed at 40 years as well as individual and continuous (residual error) level. Area under the time-concentration curve during 12-hour dosing interval ($AUC_{0\text{-}12}$) at steady state, and C_{trough} were calculated using the simulated data.

Maximum a posteriori probability Bayesian prediction

Using one concentration data for TDM, early after initiation of therapy (1, 2, 3, 4, 5, 6, 7, 8, 9, 10, 11, 12 hours after initiation of loading doses), plasma concentration over time, $AUC_{0\text{-}12}$, and C_{trough} at steady state during the maintenance therapy were predicted by MAP (maximum a posteriori) method ('MAXEVAL = 0' and 'Posthoc' in the $ESTIMATION step of NONMEM) (10-12). To mimic real clinical situation of TDM, errors in the recording of PK sampling time were also taken into account (20% for coefficient of variation).

Identification of optimal PK sampling time by evaluating predictive performance

To determine optimal sampling time for voriconazole TDM, predictability of voriconazole PK for sampling times were compared in terms of accuracy and precision. Accuracy and precision were evaluated by calculating prediction error (PE), percentage prediction error (PPE), mean of prediction error (ME), mean of percentage prediction error (MPE), root mean square error (RMSE) using the below equations.

$$\text{Prediction error} \quad (\text{PE}) = \quad Estimated\ Value - \quad Referenced\ Value$$

Percentage prediction error (PE %)

$$= 100 \times {(\text{Estimated Value} - \text{Referenced Value})}/{\text{Referenced Value}}$$

$$\text{me} = \frac{1}{N}\sum_{i=1}^{N} PE_i \;\; ; \;\; mpe = \frac{1}{N}\sum_{i=1}^{N} PPE_i \;\; ; \quad rmse = \sqrt{mse}$$

$$\text{mse} = \frac{1}{N}\sum_{i=1}^{N} (PE_i)^2 \quad , \quad rmse = \sqrt{mse}$$

Results

Simulation based on previously published PK model for voriconazole

The PK model reconstruted from the literature predicted the plasma voriconazole concentration over time reasonably well. The simulated plasma concentration profiles following each dosing scenario are shown in Figure 3. Plasma voriconazole concentration increased rapidly reaching maximum concentration at 3 hours after the initiation of loading dose. After reaching maximum concentration, plasma concentration of voriconazole rapidly decreased.

Prediction of voriconazole concentration over time by MAP method using single concentration value at various sampling times.

Plasma voriconazole concentration over time was well predicted by MAP method for all the PK sampling times explored (1 through 12 hours after the beginning of therapy during the 12-hour dosing interval) in this study (Figure 4). Bias of the predicted voriconazole concentration was within 10% for all the concentration over time profiles, for all the PK sampling time points (Figure 5). However, precision of the prediction was lower especially for the concentration around mid-points at each dosing interval (Figure 6). In scenarios 1 and 2, 95% prediction intervals (PIs) of plasma voriconazole concentration which represent the precision (reproducibility) of the Bayesian prediction during TDM were lower at the sampling time points around 4 to 6 hours as shown in Figure 6 and Appendix 1. In scenario 3, as shown in Appendix 2, 95% PI of plasma voriconazole concentration was not variable at each sampling time point.

Total exposure ($AUC_{0\text{-}12}$)

In scenarios 1 and 2, $AUC_{0\text{-}12}$ was predicted with high accuracy and precision using concentration throughout the PK sampling times but the prediction was best at 2 or 3 hour sampling time. In scenario 3, $AUC_{0\text{-}12}$ was predicted with similar accuracy using concentrations at any time point from 1 to 12 hours, but precision was predicted to be high

using concentration at around 12 hour time point. Recording error in the PK collection time did not affect the accuracy of voriconazole concentration prediction in all 3 scenarios. However, it affected the precision of the concentration prediction (Figure 7).

The 95% PIs for AUC_{0-12} were narrowest when Bayesian prediction was conducted using concentration at 7, 5, and 9 hours after dose initiation for scenario 1 through 3, respectively (Figure 7), as reflected in the smallest RMSE of 19.18, 7.10, and 7.90, respectively (Table 4).

Trough Concentration

In scenarios 1 and 2, C_{trough} was predicted with high accuracy and precision using all the PK sampling time points, but precision wass high when using concentrations at sampling time points from 6 to 8 hours. In scenario 3, C_{trough} was predicted with similar accuracy using concentrations at any time point from 1 to 12 hours, but precision was predicted to be high using concentration around 12 hours. Recording error in the sampling time did not affect the accuarcy of voriconazole C_{trough} prediction. However, it did affect the precision (Figure 8).

The 95% PIs for C_{trough} were narrowest when Bayesian prediction was conducted using concentration at 8, 9, and 10-12 hours after dose initiation for scenario 1 through 3, respectively (Figure 8), as reflected in the smallest RMSE of 0.23, 0.14, and 0.70, respectively (Table 5).

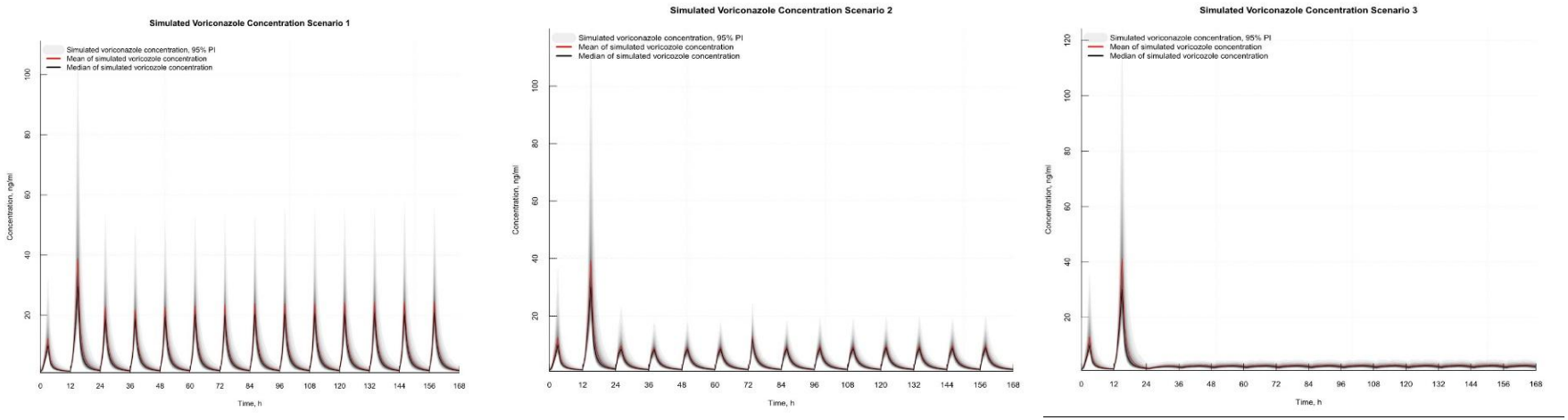

A **B** **C**

Figure 3. Simulation dataset showing simulated mean, median, 5th-pencentile, and 95th-percentile concentrations and 95% prediction intervals for voriconazole

Black solid and grey lines represent the mean and median of the simulated concentration. The band around the simulated percentiles represents the 95% confidence interval. 1,000 sets of data were simulated for each of scenario 1 (loading dose of 6 mg/kg IV q12hr and maintenance dose of 4 mg/kg IV q12hr, Figure 3A), scenario 2 (loading dose of 6 mg/kg IV q12hr and maintenance dose of 3 mg/kg IV q12hr, Figure 3B) and scenario 3 (loading dose of 6 mg/kg IV q12hr and maintenance dose of 200 mg q12hr PO, Figure 3C).

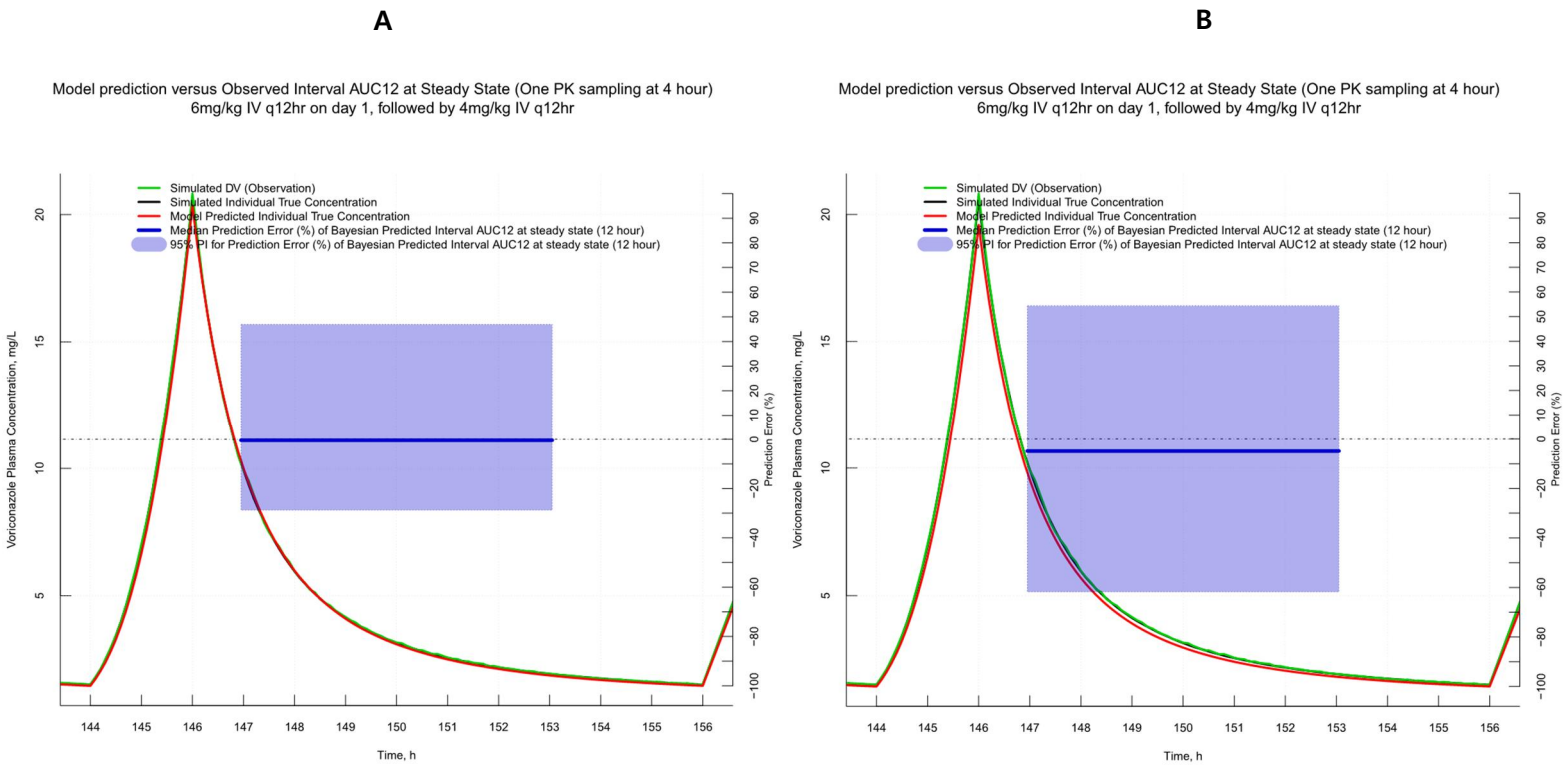

Figure 4. The plots are showing simulated value, simulated individual true value and model predicted individual value for voriconazole in sampling during loading therapy without recording error (A) and with recording error (B).

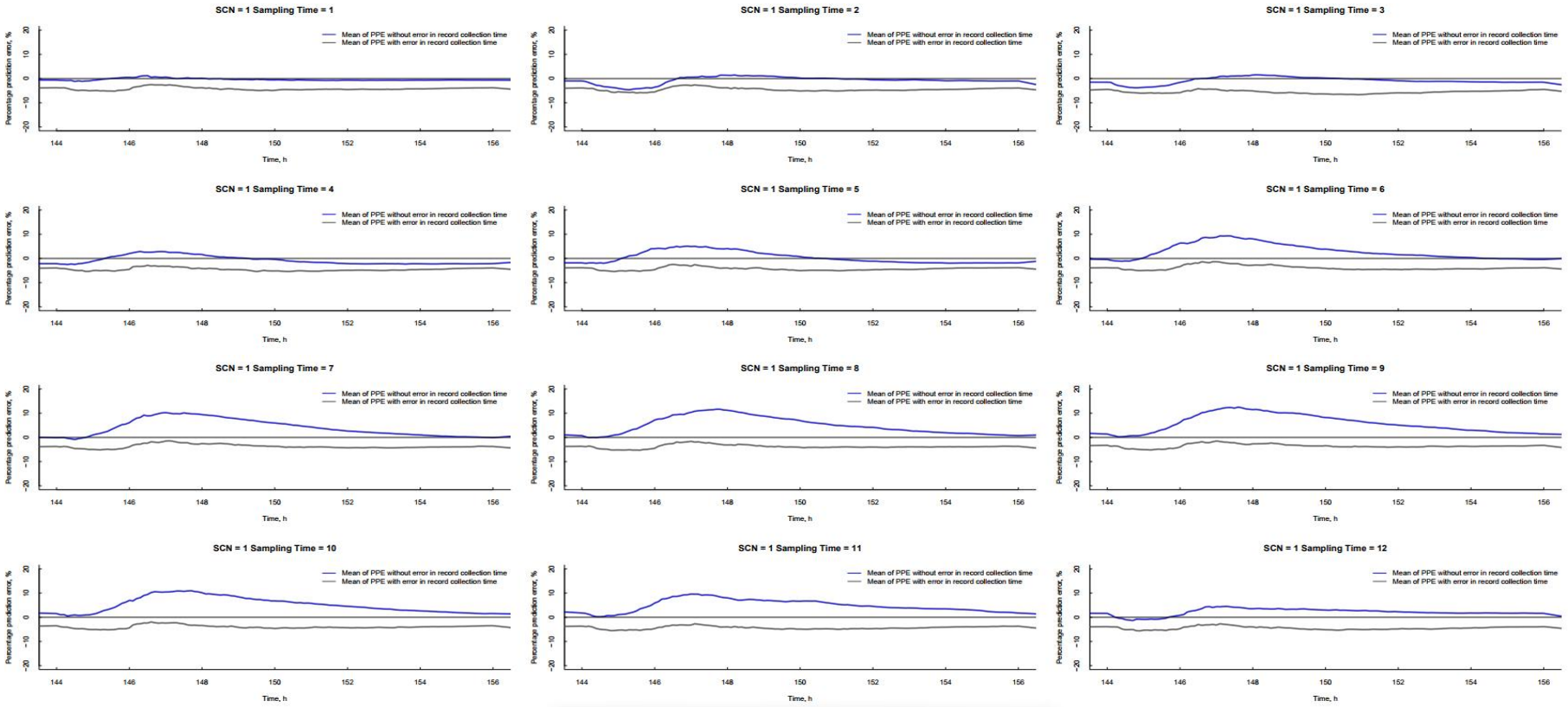

Figure 5. Accuracy of Bayesian prediction for PK voriconazole during loading therapy by sampling times at steady state for TDM (Scenario 1 as example)

The blue solid line and black solid line represent mean of percentage prediction error (PPE) for plasma voriconazole concentration without recording error and mean of PPE for plasma voriconazole concentration with recording error. The light navy band represents 95% percentile of PPE without recording error and the light black band represents 95% percentile of PPE with recording error.

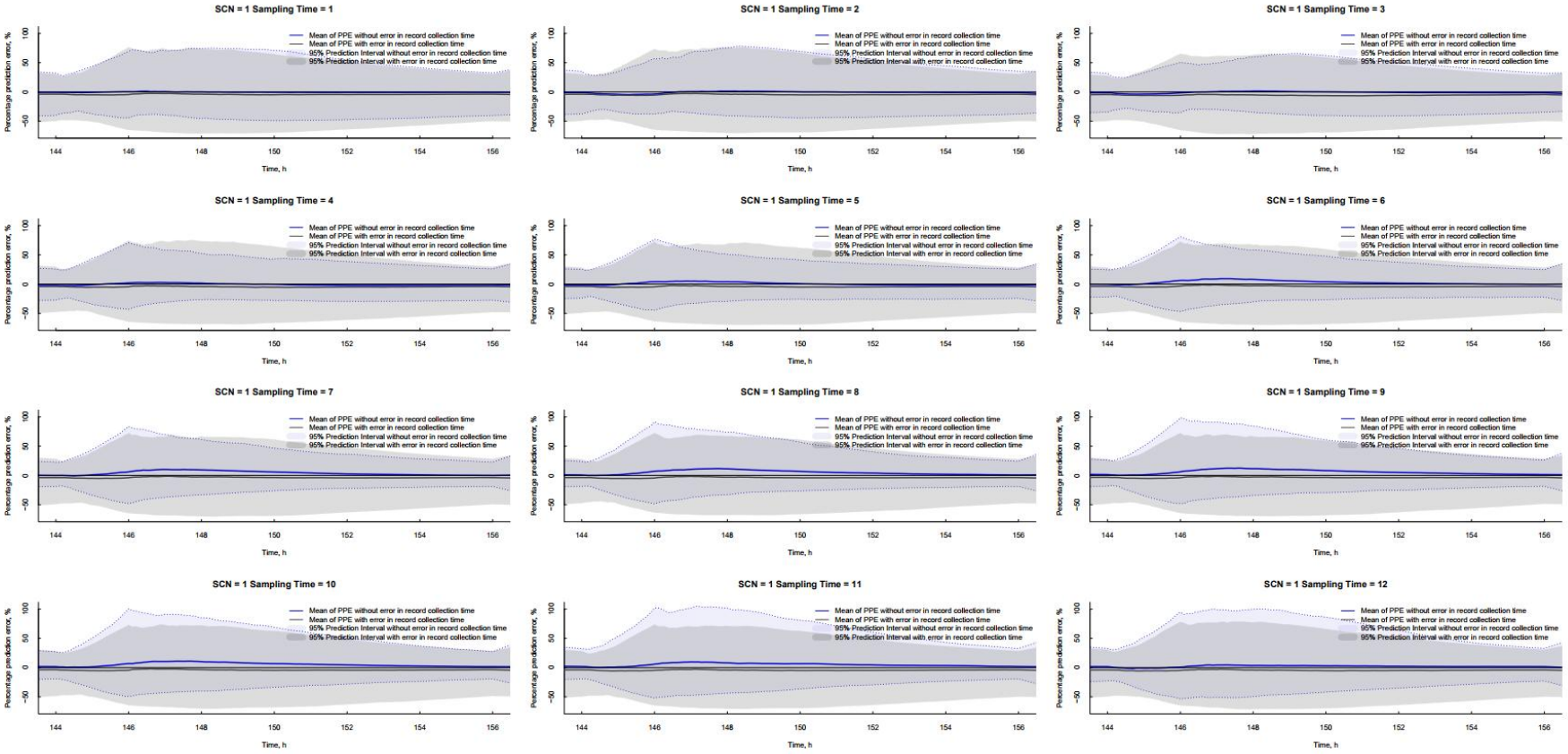

Figure 6. Accuracy and precision of Bayesian prediction for PK voriconazole during loading therapy by sampling times at steady state for TDM (Scenario 1 as example)

The blue solid line and black solid line represent mean of percentage prediction error for plasma voriconazole concentration without recording error and mean of percentage prediction error for plasma voriconazole concentration with recording error.

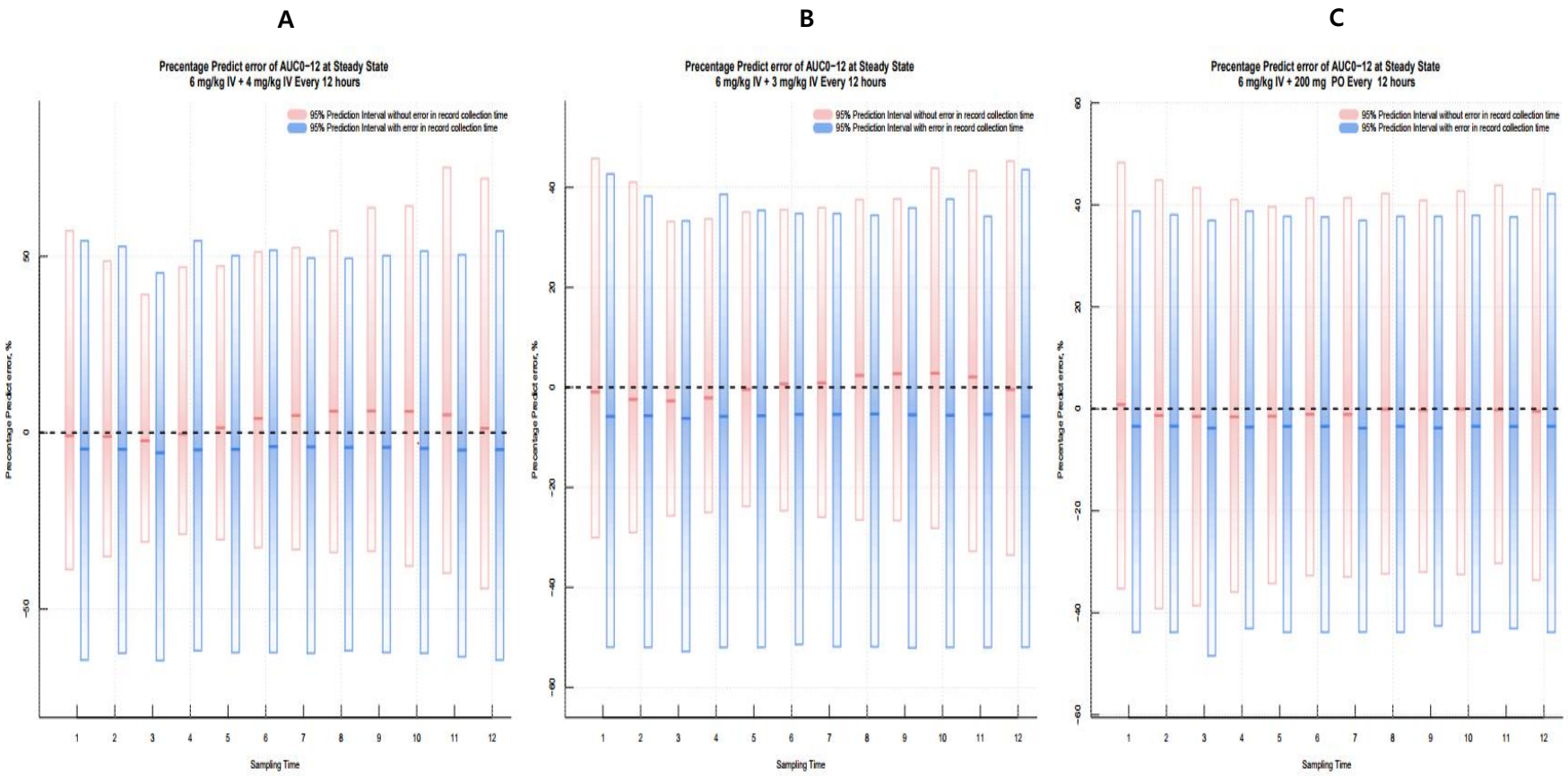

Figure 7. Accuracy and precision of Bayesian prediction for $AUC_{0\text{-}12}$ of voriconazole during loading therapy by sampling times at steady state for TDM

The red box plots represent 95% percentile of percentage prediction error for $AUC_{0\text{-}12}$ without recording error and the blue box plots represent 95% percentile of percentage prediction error for $AUC_{0\text{-}12}$ with recording error. The red and blue bands in box plots represent mean of percentage prediction error for $AUC_{0\text{-}12}$.

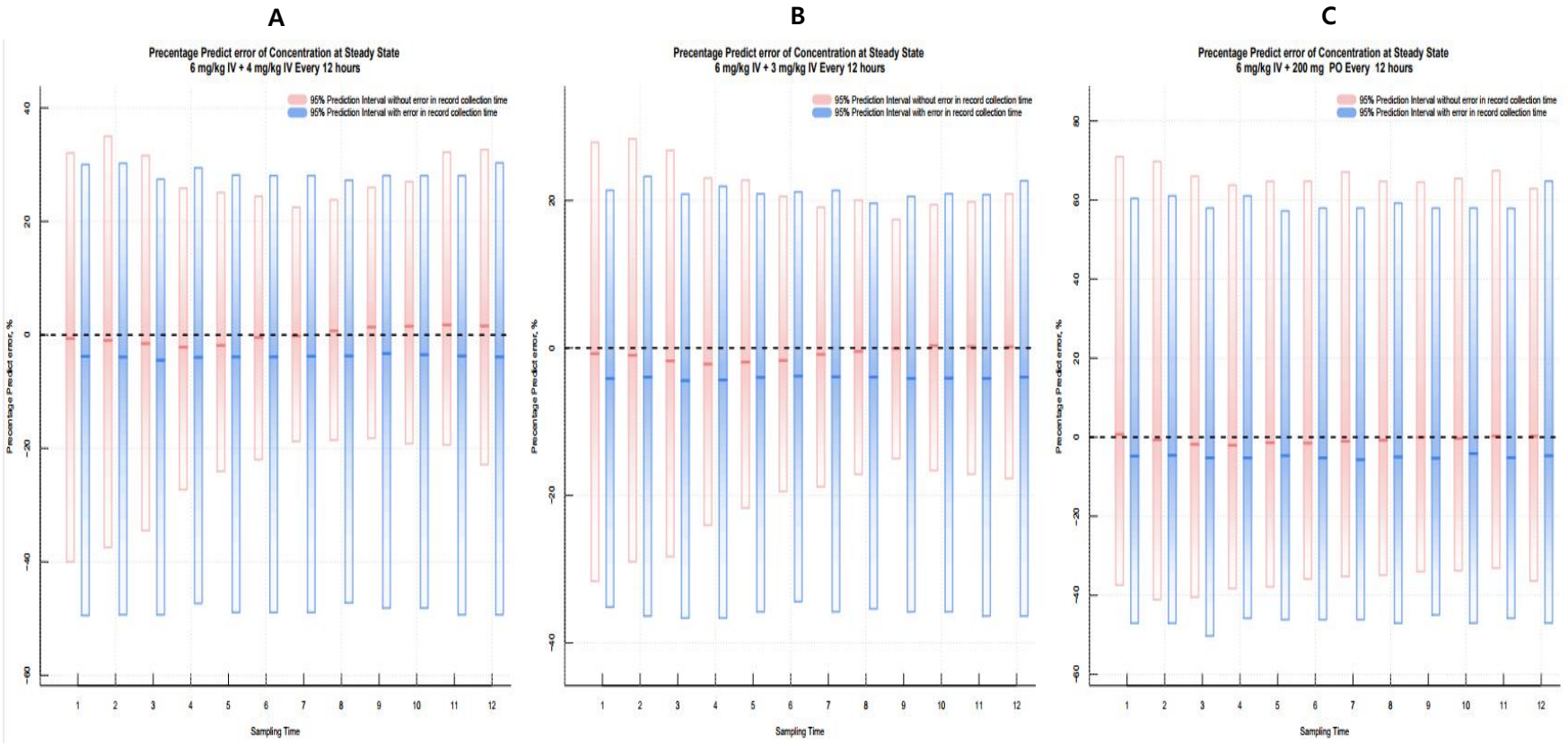

Figure 8. Accuracy and precision of Bayesian prediction for trough concentration of voriconazole after loading dose by sampling times at steady state for TDM

The red box plots represent 95% percentile of percentage prediction error for trough concentration without recording error and the blue box plots represent 95% percentile of percentage prediction error for trough concentration with recording error. The red and blue bands in box plots represent mean of percentage prediction error for C_{trough}

Table 2. Evaluation index of AUC_{0-12}

loading dose / Sampling time		Scenario 1			Scenario 2			Scenario 3		
		ME	MPE	RMSE	ME	MPE	RMSE	ME	MPE	RMSE
AUC_{0-12}	1	-5.43	1.44	55.23	-1.29	0.86	10.18	-1.23	1.80	11.12
	2	-4.93	0.09	50.17	-1.46	-0.38	9.16	-1.70	-0.09	10.65
	3	-4.26	-0.16	46.34	-1.41	-0.94	7.98	-1.74	-0.63	10.22
	4	-2.71	1.39	37.92	-0.99	-0.22	7.51	-1.55	-0.57	9.05
	5	-1.55	2.97	31.68	-0.65	0.76	7.10	-1.37	-0.30	8.66
	6	-0.09	5.01	21.76	-0.34	1.44	7.24	-1.16	0.15	8.16
	7	1.39	6.74	19.18	0.05	2.49	7.40	-0.98	0.67	8.28
	8	2.44	7.97	22.05	0.29	3.06	7.59	-0.88	0.81	7.99
	9	2.05	8.82	23.35	0.53	3.50	7.68	-0.77	1.10	7.90
	10	2.06	8.33	22.56	0.77	4.35	8.66	-0.85	1.26	8.12
	11	2.02	9.15	27.11	0.19	3.04	9.03	-0.76	1.33	8.21
	12	-0.46	5.00	26.77	-0.61	1.46	10.01	-1.00	0.56	8.14

ME: mean of prediction error; MPE: mean of percentage prediction error; RMSE: root mean square error

Table 3. Evaluation index of C_{trough}

loading dose / Sampling time		Scenario 1			Scenario 2			Scenario 3		
		ME	MPE	RMSE	ME	MPE	RMSE	ME	MPE	RMSE
C_{trough}	1	-0.11	-0.93	0.89	-0.05	-0.76	0.27	-0.07	5.87	0.93
	2	-0.10	-0.89	0.84	-0.05	-0.86	0.26	-0.10	4.22	0.90
	3	-0.10	-1.41	0.80	-0.05	-1.40	0.25	-0.10	3.63	0.87
	4	-0.08	-1.82	0.68	-0.05	-1.83	0.22	-0.09	3.44	0.79
	5	-0.07	-1.28	0.58	-0.04	-1.50	0.19	-0.07	3.75	0.76
	6	-0.04	-0.31	0.42	-0.03	-1.17	0.18	-0.05	4.29	0.73
	7	-0.02	0.61	0.28	-0.02	-0.49	0.17	-0.04	4.91	0.74
	8	0.00	1.31	0.23	-0.01	-0.06	0.15	-0.03	5.07	0.73
	9	0.00	1.87	0.33	-0.01	0.16	0.14	-0.02	5.40	0.72
	10	0.01	2.01	0.29	0.00	0.83	0.16	-0.03	5.54	0.70
	11	0.02	2.88	0.35	0.00	0.64	0.16	-0.02	5.59	0.70
	12	0.01	1.87	0.26	0.00	0.52	0.15	-0.04	4.61	0.70

ME: mean of prediction error; MPE: mean of percentage prediction error; RMSE: root mean square error

Discussion

Invasive fungal infections have a high risk of morbidity and mortality especially in immunocompromised patients. Voriconazole has a narrow therapeutic range ($1 \leq C_{trough} \leq 5.5\, ng/ml$) and $AUC_{0\text{-}12}$ (9). If plasma voriconazole concentration exceeds therapeutic range, the risk of adverse events such as visual impariment, hepatotoxicity, and cardiotoxicity increase, while therapeutic effect decreases when the concentration falls below the range. Voriconazole also has a nonlinear PK profile with high interindividual variability (13). Therefore, TDM is recommeded for voriconazole.

In this study, we found that although the accuracies of the predicted plasma voriconazole concentration over time were high, there was considerable variability in the prediction according to sampling time point with recording error for TDM (figure 5, 6), which was also the case for $AUC_{0\text{-}12}$ and C_{trough} (Figures 7, 8) as seen in the 95% PIs. These results mean that voriconazole PK prediction during TDM is not so highly reproducible, and could potentially be problematic for individualized, optimal therapy of voriconazole. Therefore, determining optimal sampling points with higher reproducible predictions should be identified scientifically to maximize the effectiveness of TDM for voriconazole. In this regard, this simulation study is helpful for individualized therapy of drugs with highly variable PK like voriconazole.

In this simulation study, prediction for the voriconazole PK during maintenance therapies were made based only on the plasma concentration during loading doses in adult patients. So further simulation study would be needed in which predictions for the voriconazole PK are made using the plasma concentration during early phase of maintenance therapy. Although the original PK model used in this simulation study encompasses many factors such as various ages from children to adults, body weight, and *CYP2C19* genotypes, the current simulations were not conducted for these factors, and done only for 40-year-old patients. These factors potentially explain the high interindividual of voriconazole PK, and this study considering

these factors could increase the accuracy and precision of the PK prediction during TDM.

Conclusion

In this study, we explored optimal sampling time for voriconazole TDM through simulation studies, where errors in the recording of the PK sampling time that may occur in the real clinical situation were also implemented. The simulation study suggested optimal sampling time point for the TDM, which will be useful for individualized, optimal therapy of voriconazole.

References

1. Pfaller MA, Pappas PG, Wingard JR. Invasive fungal pathogens: Current epidemiological trends. Clin Infect Dis. 2006;43:S3-S14.

2. Maschmeyer G, Haas A, Cornely OA. Invasive aspergillosis: epidemiology, diagnosis and management in immunocompromised patients. Drugs. 2007;67(11):1567-601.

3. Kuo IF, Ensom MH. Role of therapeutic drug monitoring of voriconazole in the treatment of invasive fungal infections. Can J Hosp Pharm. 2009;62(6):469-82.

4. Friberg LE, Ravva P, Karlsson MO, Liu P. Integrated population pharmacokinetic analysis of voriconazole in children, adolescents, and adults. Antimicrob Agents Chemother. 2012;56(6):3032-42.

5. Liu P, Mould DR. Population Pharmacokinetic Analysis of Voriconazole and Anidulafungin in Adult Patients with Invasive Aspergillosis. Antimicrob Agents Ch. 2014;58(8):4718-26.

6. Theuretzbacher U, Ihle F, Derendorf H. Pharmacokinetic/pharmacodynamic profile of voriconazole. Clin Pharmacokinet. 2006;45(7):649-63.

7. Lee J, Ng P, Hamandi B, Husain S, Lefebvre MJ, Battistella M. Effect of Therapeutic Drug Monitoring and Cytochrome P450 2C19 Genotyping on Clinical Outcomes of Voriconazole: A Systematic Review. Ann Pharmacother. 2021;55(4):509-29.

8. Elewa H, El-Mekaty E, El-Bardissy A, Ensom MH, Wilby KJ. Therapeutic Drug Monitoring of Voriconazole in the Management of Invasive Fungal Infections: A Critical Review. Clin Pharmacokinet. 2015;54(12):1223-35.

9. Patterson TF, Thompson GR, 3rd, Denning DW, Fishman JA, Hadley S, Herbrecht R, et al. Practice Guidelines for the Diagnosis and Management of Aspergillosis: 2016 Update by the Infectious Diseases Society of America. Clin Infect Dis. 2016;63(4):e1-e60.

10. Zhao W, Cella M, Della Pasqua O, Burger D, Jacqz-Aigrain E, Pediatric European Network for Treatment of Asg. Population pharmacokinetics and maximum a posteriori probability Bayesian estimator of abacavir: application of individualized therapy in HIV-infected infants and toddlers. Br J Clin Pharmacol. 2012;73(4):641-50.

11. Beal SL, Boeckmann AJ, Sheiner LB. NONMEM Users Guides. 4th ed2017 2017/04.

12. Zhao W, Elie V, Baudouin V, Bensman A, Andre JL, Brochard K, et al. Population pharmacokinetics and Bayesian estimator of mycophenolic acid in children with idiopathic nephrotic

syndrome. Br J Clin Pharmacol. 2010;69(4):358-66.

13. Yi WM, Schoeppler KE, Jaeger J, Mueller SW, MacLaren R, Fish DN, et al. Voriconazole and posaconazole therapeutic drug monitoring: a retrospective study. Ann Clin Microbiol Antimicrob. 2017;16(1):60.

국문 요약

연구목적: Voriconazole 은 침습성 진균 감염에 치료제로서 승인 받은, 대다수의 진균 및 사상균에 활성을 갖는 triazole 계열의 항진균제이다. Voriconazole은 좁은 치료역, 비선형적 약동학을 보이고, 약동학의 개인차가 크다. 이러한 이유로 voriconazole의 농도를 적정수준 범위로 유지하는 것이 침습성 진균 감염 치료에 중요하다. Voriconazole의 적정 용량 설정을 위한 약동학적 지표로는 voriconazole의 12시간 AUC (AUC_{0-12}) 와 투여 전 혈중농도 (pre-dose concentration, C_{trough})를 사용한다. 본 연구는 simulation을 수행하여 voriconazole의 치료적 약물 농도 모니터링 (therapeutic drug monitoring, TDM)을 위한 최적의 채혈시각을 제시하고자 하였다.

방법: 부하용량과 유지용량으로 구성된 Voriconazole의 적정치료 요법에 따라 세 가지의 투여 시나리오를 구성하여, 각 시나리오에서 시간에 따른 voriconazole 농도를 각각 1,000회의 Monte-Carlo 시뮬레이션에 의해 생성하였다. 시뮬레이션된 voriconazole의 혈중농도 중 첫 부하용량 투여 후 1 ~ 12시간에 해당되는 농도 데이터를 각각 선택해 해당 농도를 사용하여 Maximum a posterior (MAP) 방법을 사용하여 유지용량에서의 항정상태 voriconazole의 혈중농도를 예측하였으며, 이를 해당 시점의 시뮬레이션 값 (참값)과 비교함으로써 최적의 농도 채혈시각을 추정하였다. 시뮬레이션 시 채혈 기록의 오류를 반영하기도 하였으며, 베이지안 추정에 사용된 집단약동학모델은 기존의 문헌을 참고하여 NONMEM으로 재구성 하였고, 예측한 유지용량에서의 농도와 시뮬레이션 값을 위한 추정된 농도의 정확도와 정밀도 측면에서 비교하였다. 모든 수행 과정은 NONMEM (version 7.4) 과 R software (version 3.6.3)를 이용해 수행하였다.

결과: 예측된 voriconaozle의 혈중농도는 모든 채혈시각에서 높은 정확도 (오차 ±10%) 을 보였으나 정밀도는 각 채혈시각에 따라서 상이하였다. 채혈기록 오류를 반영한 시뮬레이션에는 반영하지 않은 경우에 비해 정확도 및 정밀도가 떨어지는 것을 확인할 수 있었다.

결론: 이번 연구를 통해 voriconazole의 TDM 수행 시, 최적의 약동학 채혈시각을 제시할 수 있었으며 채혈시각에 대한 기록 오류가 발생했을 시 정밀도의 감소에 따라 개별 환자의 voriconazole의 혈중농도 예측의 오류가 생길 수 있으므로 정확한 약동학적 채혈시각의 기록이 중요함을 알 수 있었다.

Appendix

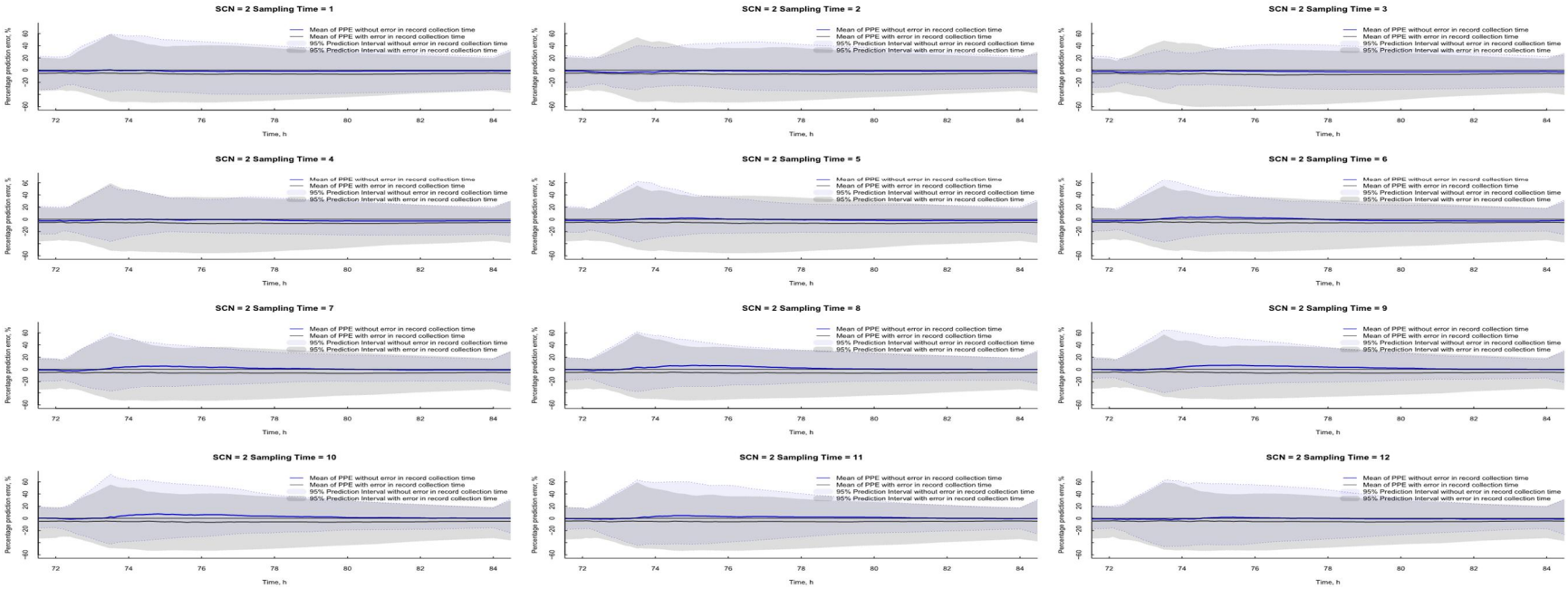

Appendix. 1 Accuracy and precision of Bayesian prediction for PK voriconazole during loading therapy by sampling times at steady state for TDM (Scenario 2)

The blue solid line and black solid line represent mean of percentage prediction error (PPE) for plasma voriconazole concentration without recording error and mean of percentage prediction error for plasma voriconazole concentration with recording error. The light navy band represents 95% percentile of PPE without recording error and the light black band represents 95% percentile of PPE with recording error.

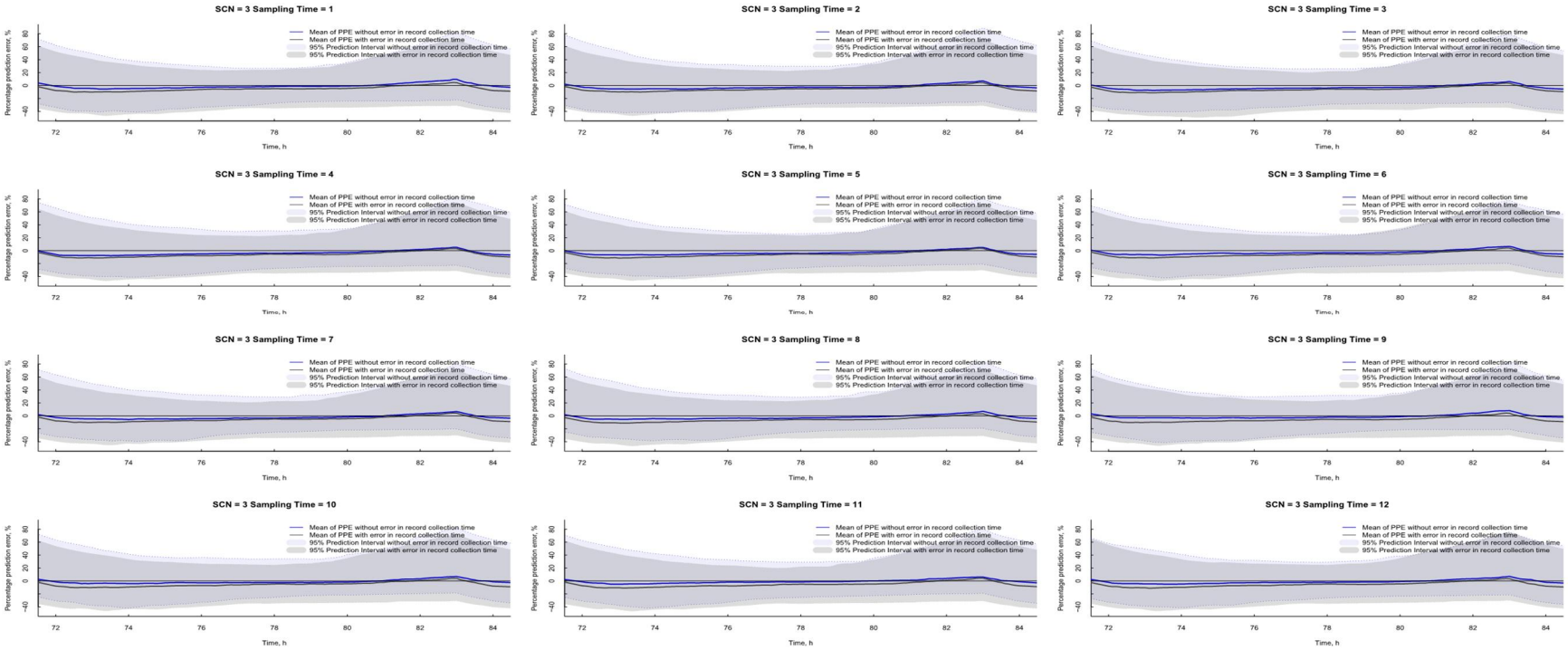

Appendix. 2 Accuracy and precision of Bayesian prediction for PK voriconazole during loading therapy by sampling times at steady state for TDM (Scenario 3).

The blue solid line and black solid line represent mean of percentage prediction error (PPE) for plasma voriconazole concentration without recording error and mean of percentage prediction error for plasma voriconazole concentration with recording error. The light navy band represents 95% percentile of PPE without recording error and the light black band represents 95% percentile of PPE with recording error.